Control of inflorescence architecture in *Antirrhinum*

Desmond Bradley, Rosemary Carpenter, Lucy Copsey, Coral Vincent, Steven Rothstein* & Enrico Coen

Genetics Department, John Innes Centre, Colney Lane, Norwich NR4 7UH, UK

Flowering plants exhibit two types of inflorescence architecture: determinate and indeterminate. The *centroradialis* mutation causes the normally indeterminate inflorescence of *Antirrhinum* to terminate in a flower. We show that *centroradialis* is expressed in the inflorescence apex a few days after floral induction, and interacts with the floral-meristem-identity gene *floricaula* to regulate flower position and morphology. The protein CEN is similar to animal proteins that associate with lipids and GTP-binding proteins. We propose a model for how different inflorescence structures may arise through the action and evolution of *centroradialis*.

PLANTS exhibit highly varied architectures, from simple stems terminating in a flower to large, highly branched structures[1]. This variation is largely dependent upon where and when flowers are made[2–4]. In plants with determinate inflorescences the main axis of growth terminates in a flower, and further flowers are produced by branching events that occur below this. In species with indeterminate inflorescences, the main axis is prevented from forming a flower and can therefore grow indefinitely, allowing more flowers to form on an elongated stem (illustrated by the wild-type *Antirrhinum* inflorescence in Fig. 1). Evolution is thought to have proceeded from determinate to indeterminate growth, presumably by recruiting genes that repress the formation of terminal flowers[5,6]. The *centroradialis* (*cen*) mutation of *Antirrhinum* causes the inflorescence to terminate in a flower, confering the determinate condition (Fig. 1)[7,8]. To understand how the formation and repression of flowers are coordinated to give a particular plant architecture, we have analysed the mechanism by which *cen* acts.

In *Antirrhinum*, the apical meristem of the primary shoot first undergoes a vegetative phase, generating leaf primordia on its flanks that bear secondary shoot meristems in their axils (the region between the stem and leaf). Under the appropriate developmental and environmental signals, such as long day length, the apical meristem is converted to an inflorescence meristem[2,9], which produces modified leaf primordia (bracts) with floral meristems in their axils. The apical meristem maintains its inflorescence identity throughout the remainder of its lifetime, generating flowers in axillary positions (Fig. 1). This pattern is reflected in the expression of floral-meristem-identity genes such as *floricaula* (*flo*) and *squamosa* (*squa*), which are expressed in floral meristems and their subtending bracts but not in the apical meristem[9–11,33]. Floral meristems give rise to four concentric whorls of organs: five sepals outermost, surrounding five petals which are united for part of their length, followed by four stamens and the central two fused carpels. *Antirrhinum* flowers are zygomorphic, having a single plane of symmetry[12,13].

The cen mutant of *Antirrhinum* differs from wild type in several key respects. (1) The mutant produces a terminal flower, converting the inflorescence from indeterminate to determinate (Fig. 1). Consequently, the architecture is changed to a shorter, more bushy plant, as shoots cannot grow indefinitely. (2) About 10 axillary flowers are made below the terminal flower, indicating that there may be a delay in switching from an inflorescence to a floral meristem (see legend to Fig. 1). (3) The terminal floral meristem is developmentally more advanced than the axillary flowers below it. (4) Unlike axillary flowers, organ numbers and their arrangement (phyllotaxy) are very variable in terminal flowers (Fig. 1). (5) The terminal flower is usually radially symmetrical, with all petals resembling the ventral (lowest) petal of axillary flowers. Together, these five aspects of the cen mutant phenotype indicate a primary role for *cen* in the programming of the apical meristem and key interactions with floral-meristem-identity genes. Mutants have also been described in *Digitalis* and *Arabidopsis* that convert an indeterminate to a determinate meristem with the production of a terminal flower[14–16]. The

FIG. 1 Inflorescences of wild-type *Antirrhinum* (left) and the cen mutant (right). The number of axillary flowers below the terminal flower ranged from 6 to 16 for the main stem, and 4 to 15 for secondary branches; 439 inflorescences were scored from 11 different families carrying the *cen*-594, *cen*-663 or *cen*-665 alleles. Although terminal flowers often had the same number of organs as axillary flowers, there was variation, from 3 to 8 sepals and 4 to 9 petals in the terminal flowers of secondary branches. The number of stamens also varied and these were often petaloid. Greater variation was observed in the terminal flowers of the main stem than in those of secondary branches.

* Present address: Department of Molecular Biology and Genetics, University of Guelph, Guelph, Ontario, N1G 2W1 Canada.

other aspects of the cen mutant phenotype are also seen in the cen-like mutants of these species. An additional feature of the *Arabidopsis* mutant, *terminal flower* (*tfl*), is that it flowers earlier than wild-type plants.

Here we describe the molecular and morphological analysis of cen mutants, showing when and where *cen* acts in relation to flowering. The protein CEN has some similarities to a family of phosphatidylethanolamine-binding proteins (PBPs) found in animals; PBPs are thought to interact with membranes and possibly GTP-binding proteins[17,18]. In wild type, *cen* is most strongly induced in the region just below the shoot apical meristem, and may act cell-non-autonomously to prevent *flo* expression in the apex. By analysis of *flo* and *cen* induction, we suggest a model that explains the architectures and floral morphologies of both the wild type and cen mutant of *Antirrhinum*.

Morphology and development of cen mutants

To understand how and when *cen* acts in relation to inflorescence and floral induction, we analysed the morphological development of cen mutant inflorescences by using scanning electron microscopy (SEM). Three aspects of the terminal flower of cen mutants were investigated: phyllotaxy, organ number, and developmental age in comparison to axillary flowers. SEM analysis of wild-type plants has defined several morphologically distinct stages of floral meristem development[11]. Stage 0 is marked by the presence of small bract primordia arising on the flank of the apex. At stage 1, floral meristems comprise an eye-shaped group of cells lying in the axil of a bract. At stage 2, floral meristems are raised up to give a loaf-like appearance. By late stage 2, the floral meristem is distinguishable from a vegetative meristem by its larger size and rounder shape. By stage 3, the pentagonal shape of the floral meristem is clear, and by stage 4 the sepal primordia are visible. Plants mutant for *cen* were grown under short days to maintain vegetative growth, and were switched to long days to induce inflorescence and floral development. Apices of plants collected on 0, 4, 6, 7, 8 or 10 days after induction were analysed by SEM (Fig. 2). One set of plants was left to mature in long days and produced 10 (±1) axillary flowers below the terminal flower.

Under SEM, cen mutant plants collected 4 days after induction looked similar to plants at day 0, with the youngest bract primordia arising sequentially in a spiral on the flanks of the inflorescence meristem (Fig. 2). By day 6, axillary meristems could be distinguished as either vegetative or floral (Fig. 2). The lowest floral meristem was labelled flower 1, and all meristems above it were numbered sequentially. Flower 1 was at about stage 2–3 on day 6 and had about 11–12 primordia above it. Because only 10 flowers were eventually produced, the youngest one or two primordia at the apex are thought to have become the sepals of the terminal flower. By day 7, a morphological change was clearly detectable in the terminal meristem that distinguished it from a normal inflorescence apex. At this stage, all ten axillary floral meristems could be identified, each in the axil of a bract. The terminal meristem was more advanced than any of the axillary floral meristems, with larger sepal and petal primordia visible; the terminal meristem was at about stage 4, whereas flower 1 was at stage 3. The sepals of the terminal meristem did not usually arise simultaneously in a whorl, as seen in axillary meristems (for example, flower 1), but were most often in a spiral, sometimes as two whorls of three, or

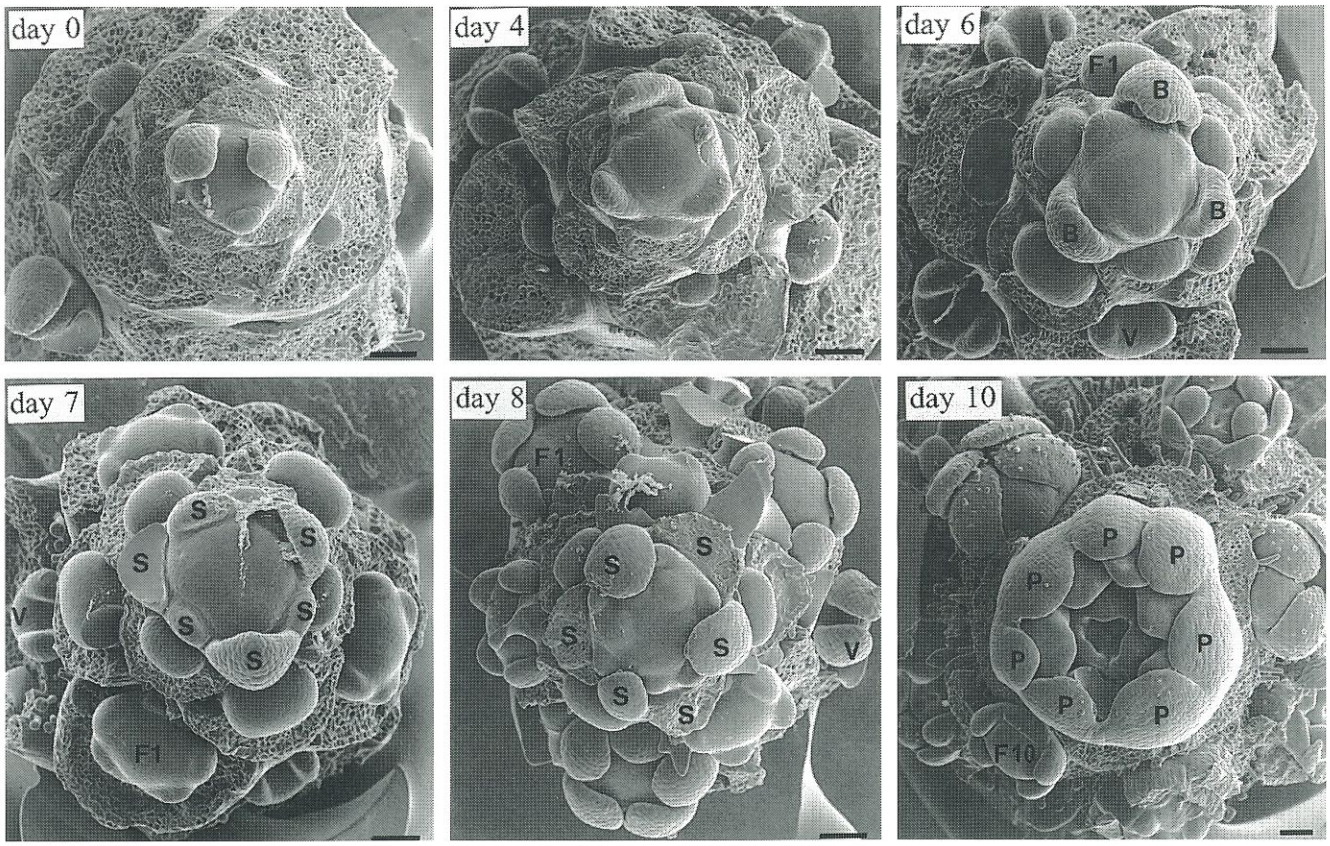

FIG. 2 Inflorescence development in the *cen* mutant of *Antirrhinum*. SEMs were made of inflorescence apices, collected on day 0, 4, 6, 7, 8 or 10 after plants were switched to long days to induce flowering. Flowers were numbered sequentially, flower 1 (F1) being the lowest and F10 residing just below the terminal flower. The sepals (S) and petals (P) are indicated for the terminal flower, some of which removed to reveal changes occuring in the inner whorls. Bracts (B) were also removed from most axillary flowers to reveal the developing meristem. Scale bars, 100 μm.
METHODS. Induction of flowering used plants carrying the *cen*-663 allele (JI.663) and was performed as described in Fig. 3. SEMs were made from plastic replicas[28].

even as a whorl of four together with one or two individual primordia. By day 8, the terminal floral meristem had clear sepal, petal and stamen primordia, whereas the petal and stamen primordia were only just apparent in the oldest axillary floral meristem. The terminal meristem usually had six sepals, most commonly arranged in a spiral.

The terminal flowers of plants analysed under SEM showed some variation in organ numbers, reflecting differences seen in plants left to mature; 6 ± 1 sepals (range 4–7). Although petal numbers also showed a small variation, they usually arose in a whorl (Fig. 2). At later stages of development, the terminal floral meristem often had five or six stamens internal to the petals, and usually two fused carpels, although three could sometimes occur.

The terminal floral meristem, therefore, behaved similarly to an axillary floral meristem; it developed at about the same rate as the axillary floral meristems (always being about one developmental stage ahead of flower 1 at any given time), and it usually made a similar number of organs to the axillary flower.

Expression of *flo* in the cen mutant

Two explanations might account for the more advanced nature of the terminal meristem: either it was initiated slightly earlier than flower 1, or it was recruited to form a flower at a more advanced stage of development. These two possibilities were tested by analysing *flo* expression. In wild-type apices, *flo* is activated in the youngest primordia flanking the apical meristem (stage 0), within 1–2 days of floral induction, and is an early marker for commitment to floral meristem identity[33]. We therefore compared *flo* induction in the cen mutant with wild type to determine its time of activation in the apex, and whether its expression domain or time of induction were consistent with the cen phenotype.

Wild-type and cen mutant plants were kept in short-day conditions to maintain vegetative growth before switching to long days to induce flowering. Apices were collected on days 0, 1, 2, 3, 4, 6, 7, 8 or 10 (long days) for RNA *in situ* hybridization (Fig. 3). Similar to wild-type plants, *flo* was induced after 1–2 long days in *cen* mutants in the youngest bract primordia arising from the flanks of the apical meristem (data not shown). Between days 0 and 4, about 5–7 bract primordia were initiated that expressed *flo*, and floral meristems at about stage 1 could be distinguished in the axils of older bracts (Fig. 3*a*). No expression of *flo* was observed in the apical meristem of cen mutants until day 6, after which *flo* expression was observed throughout the apical meristem (Fig. 3*b*). Wild-type control plants studied at this or any later time point after induction did not show any *flo* expression in the apical meristem (Fig. 3*c*; an example of wild type 6 days after induction). The ectopic expression of *flo* in the cen mutant shows that *cen* normally prevents *flo* expression in the apex.

According to SEM of cen mutants, the youngest primordia flanking the apex by day 6 would form the sepals of the terminal flower, so that it was similar to about a stage 3–4 floral meristem. Consistent with this, the expression pattern of *flo* in the apical

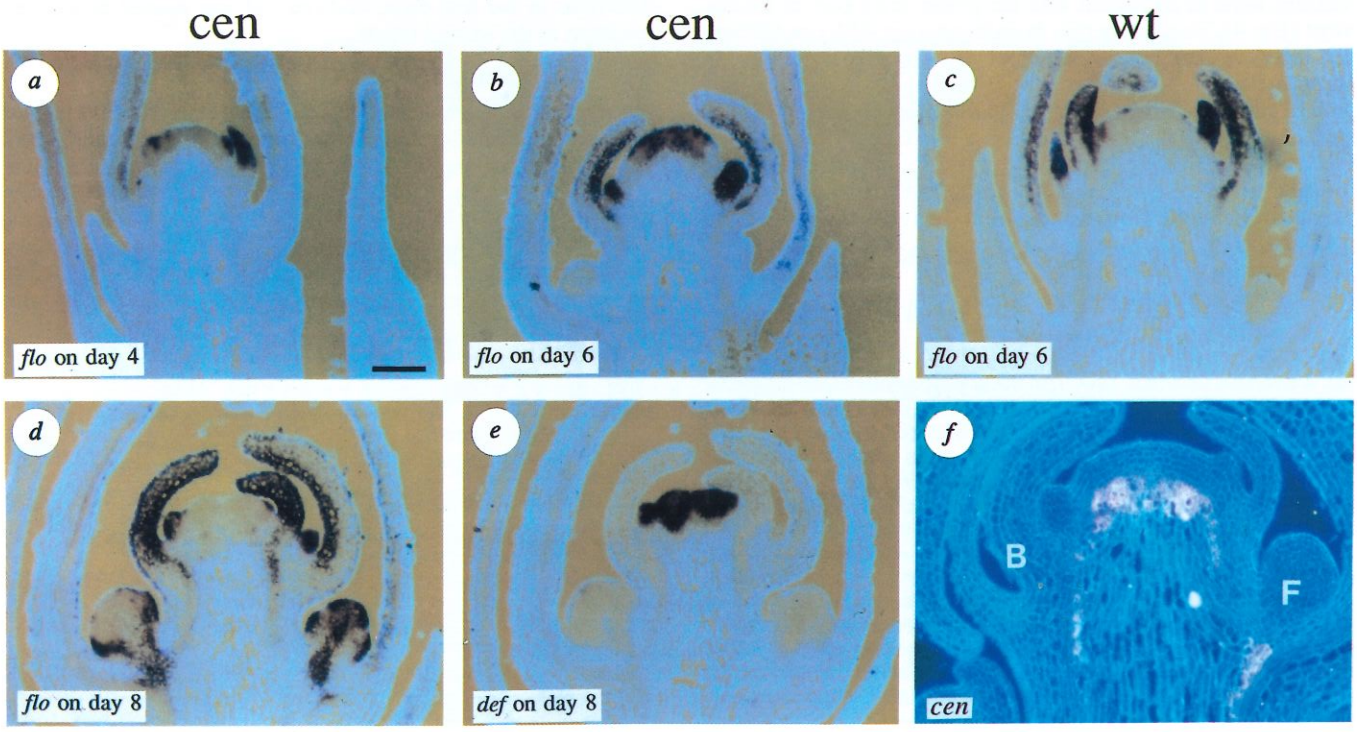

FIG. 3 RNA *in situ* hybridizations with *flo*, *def* and *cen*. *a*, *b* and *d*, Expression of *flo* in the cen mutant of *Antirrhinum* collected on day 4, 6 or 8, respectively, after floral induction. (Note that the more domed shape of the apex in *b*, compared to *a* or *d*, was due to the plane of section.) *c*, Expression of *flo* in a wild-type (wt) inflorescence on day 6. *e*, Expression of *def* in the cen mutant on day 8. Longitudinal sections of inflorescences were probed with digoxigenin-labelled antisense RNA. When viewed under light-field the RNA signal is purple on a white tissue background. Plants were grown under short-day conditions to prevent inflorescence development and then switched to long days to promote flowering. *f*, Expression of *cen* in wild-type (wt). Apices of mature wild-type inflorescences were collected from the field and probed for *cen* expression. When viewed under dark-field the RNA signal is a bright pale pink/orange colour on a blue tissue background. All sections are at the same scale; scale bar, 100 μm. Note that apices of *cen* mutants were morphologically similar to wild type until about day 6–7 (see Fig. 2).

METHODS. For *a*–*e*, cen mutant plants (JI.663) or wild type (JI.2) were grown under environmentally controlled conditions at about 200 microEinsteins (μE) $s^{-1}m^{-2}$ and 25 °C for about 40 short days (8 h light : 16 h dark) before changing to long days (16 L : 8 D). Plants were collected on the day before the change day (day 0) or on subsequent days after exposure to the extended day length. The *flo* and *def* probes and methods for digoxigenin labelling of RNA probes, tissue preparation and *in situ* hybridization were as described previously[9,20]. An internal *Acc*I–*Rsa*I fragment of the partial *cen* cDNA pJAM2020 was subcloned in to Bluescript vector KS+ and used to generate antisense and sense control probes using T3 and T7 polymerases.

meristem on day 6 was typical of a stage 3–4 floral meristem. To determine the developmental stage of the terminal meristem, consecutive sections of apices were probed for expression of *flo* or the floral-organ-identify gene *deficiens* (*def*), which is first expressed at about stage 3–4 in axillary meristems[19,20] By day 7, *flo* expression was maintained throughout the apical meristem, while the *def* gene was expressed in the centre of the terminal meristem and was not detected in any axillary meristem (data not shown). After 8 days, the pattern of *flo* expression in the terminal meristem was typical of a stage 4–5 floral meristem (Fig. 3*d*). By 8 days, the expression of *def* was more extensive in the apical meristem and just visible in the oldest axillary floral meristem, flower 1 (Fig. 3*e*). These results suggest that the apical meristem of the cen mutant was recruited at a late stage (stage 2–3) to floral development, thus appearing more advanced than any axillary meristem.

Isolation of *cen*

To study the molecular action of *cen* and its relationship to inflorescence development, we isolated *cen* by transposon-tagging. Transposon-induced mutations of *cen* were obtained by crossing transposon-active lines to a line carrying the classical *cen* allele, *cen*-594 (refs 7, 8). By this strategy, 8,339 F_1 plants were screened and three new alleles of *cen* (*cen*-663, *cen*-665 and *cen*-666) were obtained. A Tam6 probe identified a 6.0-kb band that was uniquely present in *cen*-663 and linked to the cen phenotype. The DNA fragment was cloned, mapped and a flanking region used to probe DNA from different *cen* mutants and wild-type siblings, all heterozygous for *cen*-594 (Fig. 4). The restriction patterns were all consistent with the probe being part of the *cen* locus (Fig. 4). To confirm this, homozygous *cen*-594, *cen*-663 and *cen*-665 were grown and self-pollinated at 15 °C to induce transposon excision[21]. A small proportion of progeny from these self-pollinated plants were found with a revertant wild-type phenotype, indicating that these alleles were genetically unstable, as expected if they were caused by a transposon insertion. The revertants in each case had a restored wild-type band of 6.5 kb, presumably due to transposon excision (Fig. 4).

Overlapping clones from a wild-type genomic library were isolated using the 2-kb flanking probe and used to construct a map of the *cen* region (Fig. 5*a*). A wild-type 6.5-kb *Eco*RI fragment was subcloned and fully sequenced. The insertions causing the different *cen* alleles were first mapped by genomic DNA blots. This indicated that an *Acc*I–*Eco*RI fragment at the right-hand end of the 6.5-kb *Eco*RI fragment was critical to *cen* function. However, when this and other fragments of the 6.5-kb *Eco*RI clone were used to probe a complementary DNA-library made from poly(A) RNA from inflorescences of wild-type *Antirrhinum*, no hybridizing clones were detected, presumably due to the low abundance of *cen* RNA. About 200 bp flanking the *cen*-663 allele were sequenced, and several oligonucleotides based on this sequence were used in reverse transcription–polymerase chain reaction (RT–PCR) on total RNA from young inflorescences of wild-type *Antirrhinum* or *cen* mutants. Only oligonucleotides pointing left to right, 5′ to 3′ in Fig. 5, gave a PCR product (in combination with an oligonucleotide designed to hybridize with the poly(A) tail). No PCR product was detected using RNA from the *cen* mutants.

A PCR cDNA was isolated, sequenced and compared to the genomic region to determine the intron–exon boundaries. The 5′ end of the *cen* mRNA was determined by 5′ RT–PCR, and the complete cDNA and open reading frame (ORF) determined (Fig. 5*b*, *c*). The gene consisted of four exons comprising about 980 bp. The ORF could encode a 181-amino acid protein of relative molecular mass 20,300 (M_r 20.3K). No obvious structural motifs were found in the protein CEN using standard programs[22]. Using a conserved oligonucleotide to the CACTA end of a family of transposons in *Antirrhinum*, in combination with oligonucleotides to the *cen* region, the different *cen* alleles were mapped precisely (Fig. 5*b*). Two alleles, *cen*-663 and *cen*-665, were caused by Tam insertions in the first exon, and *cen*-594 was caused by a Tam4 insertion in the second intron.

Proteins similar to CEN

Database searches indicated that the CEN protein had highest similarity to a family of phosphatidylethanolamine-binding proteins present in animals, isolated based on their affinities to organic anions or lipids, or through their association with membrane–protein complexes (Fig. 5*d*)[17,18]. The similarity extended throughout the proteins, and a potential nucleotide-binding region was partly conserved (CEN residues 116–132). Biochemical evidence suggests that these proteins may also

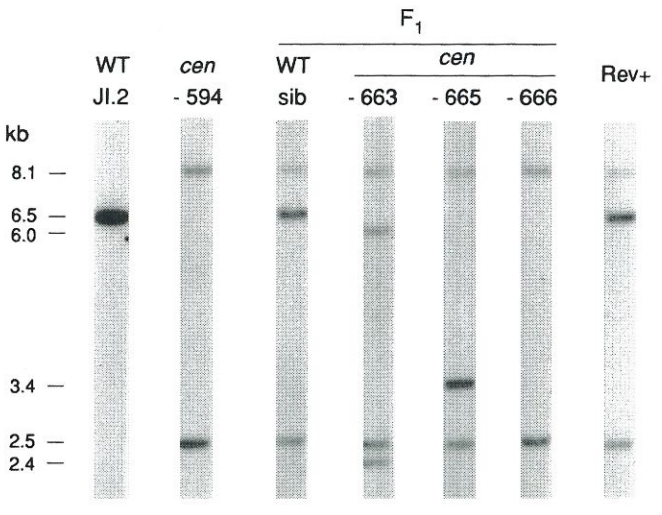

FIG. 4 Genomic DNA blot. DNA from the wild-type *Antirrhinum* progenitor line JI.2 (WT), the *cen* allele (*cen*-594) from the Gatersleben collection, Germany[34], and three new *cen* alleles (*cen*-663, *cen*-665, and *cen*-666) identified in the F_1 population arising from a cross between mutagenized JI.2 plants crossed to *cen*-594, were digested with *Eco*RI, blotted and probed with the blanking region of pJAM2017 (see Fig. 5 for map). A wild-type F_1 sibling (WT sib) arising from the mutagenesis and a wild-type revertant (Rev+) arising from the *cen*-594 allele were treated similarly. The wild-type progenitor gave a 6.5-kb band, whereas the *cen*-594 mutant, used as one parent in the tagging experiment, gave 8.1-kb and 2.5-kb bands. As expected, wild-type F_1 plants (*cen*-594/*Cen*$^+$) had all three bands (see WT sib in Fig. 4). The three F_1 cen mutants had lost the wild-type 6.5-kb band, but all mutants had the 8.1-kb and 2.5-kb bands derived from the *cen*-594 parent. In *cen*-663, a 6.0-kb band was detected, equivalent to that cloned (variable levels of a 2.4-kb band were also observed; see legend to Fig. 5). The *cen*-665 mutant had a new band of 3.4 kb. The *cen*-666 allele had neither the wild-type nor any new band, and was never obtained in a homozygous state, suggesting that it carried a large and possibly lethal deletion.

METHODS. The original *cen* allele, *cen*-594, was obtained from Gatersleben[7,8,34]. A line derived from wild-type JI.2 was grown at 15 °C and then crossed with *cen*-594. F_1 progeny (8, 339) from these crosses were grown and three new *cen* alleles, *cen*-663, *cen*-665 and *cen*-666, were obtained. These F_1 plants and three wild-type siblings from each family were maintained as cuttings for self-pollinating and crossing. Genomic DNA from each F_1 *cen* mutant and three wild-type siblings were probed with fragments of transposons Tam1–Tam8 to find any new insertion unique to each allele. A second screen of these new insertions was made on populations segregating for each *cen* allele to establish linkage with the cen mutant phenotype. A Tam3 insertion provided an independent restriction fragment length polymorphism (RFLP) marker for distinguishing plants carrying *cen*-594 from the other alleles (data not shown). The individual *cen* alleles were obtained by backcrossing the F_1 *cen* mutants to wild type and selecting progeny, using the RFLP marker, that carried the new alleles. These were self-pollinated, and the segregating progeny were tested for linkage of new insertions with the cen phenotype. Growth of plants and methods for DNA extraction and blot analysis were as described previously[12,20].

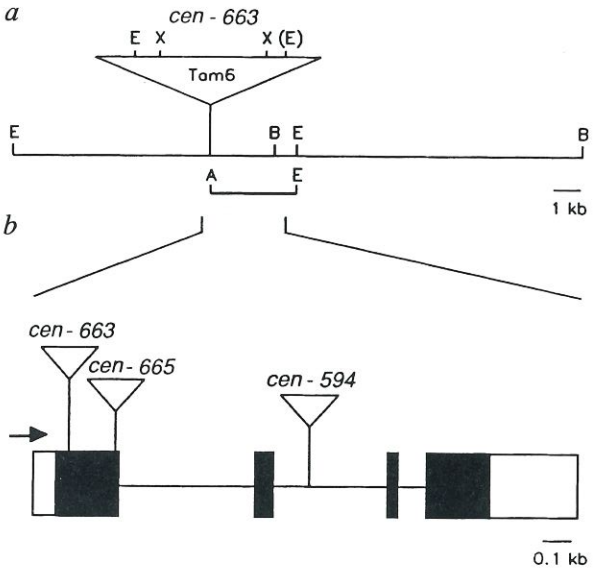

c

```
1                                                aagcaacatcaaaaacagcatcataaatcct   31
32   tttacttttgttgcatttttatcatcttaattaagcattcttctccatataatatagtt   90

91   atg gca gca aaa gtt tca tcg gac ccg cta gtg ata ggg aga gtt   135
     Met Ala Ala Lys Val Ser Ser Asp Pro Leu Val Ile Gly Arg Val

136  atc gga gac gtt gtt gat cat ttt acc tca act gtt aaa atg tct   180
     Ile Gly Asp Val Val Asp His Phe Thr Ser Thr Val Lys Met Ser

181  gtt att tac aac tcc aac aat tcc atc aag cat gtc tac aat ggc   225
     Val Ile Tyr Asn Ser Asn Asn Ser Ile Lys His Val Tyr Asn Gly

226  cat gag ctc ttt cct tcc gct gtt acc tct aca cct agg gtt gag   270
     His Glu Leu Phe Pro Ser Ala Val Thr Ser Thr Pro Arg Val Glu

271  gtt cat ggt ggt gat atg aga tca ttt ttc act ctg ata atg aca   315
     Val His Gly Gly Asp Met Arg Ser Phe Phe Thr Leu Ile Met Thr

316  gac cct gat gtt cct ggt cct agt gat cca tac ctg agg gag cac   360
     Asp Pro Asp Val Pro Gly Pro Ser Asp Pro Tyr Leu Arg Glu His

361  ttg cac tgg ata gtc aca gat atc cca ggg acc act gat tcc tca   405
     Leu His Trp Ile Val Thr Asp Ile Pro Gly Thr Thr Asp Ser Ser

406  ttc ggc aaa gaa gta gtg agc tat gag atg cca agg ccg aac ata   450
     Phe Gly Lys Glu Val Val Ser Tyr Glu Met Pro Arg Pro Asn Ile

451  ggg atc cac agg ttt gta ttt ctt ctg ttc aaa cag aag aaa aga   495
     Gly Ile His Arg Phe Val Phe Leu Leu Phe Lys Gln Lys Lys Arg

496  ggg cag gcg atg ttg agc cca cca gta gtg tgc agg gat gga ttc   540
     Gly Gln Ala Met Leu Ser Pro Pro Val Val Cys Arg Asp Gly Phe

541  aac acg aga aaa ttc aca cag gaa aat gaa ttg ggc ctc cct gtt   585
     Asn Thr Arg Lys Phe Thr Gln Glu Asn Glu Leu Gly Leu Pro Val

586  gcc gct gtc ttc ttc aat tgc cag cgc gaa acc gct gcc aga agg   630
     Ala Ala Val Phe Phe Asn Cys Gln Arg Glu Thr Ala Ala Arg Arg

631  cgt tga acgtactatttatccatatcttatggctctgcatatatatatatatatatg   687
     Arg  *

688  ctagtactactgatgtatcttcatcagggaaataaatcatatgtagggtttcttttgca   746
747  atgataaagagtccctacgtctgctaccaaaaaaaaattgttagagtggcctttgcaagt   805
806  agtgaaaggatatgtgtacgtaatagggaaggaaaagatggagaaatgggaaattgtga   864
865  tgtccacttgttataaattgatgtaattaatttctatgatatatatatttggaagttgtg   923
924  ttgtgc                                                         929
```

d

```
CEN  VYNGHELFPSAVTSTP..RVEVHGGDMRSFFTLIMTDPDVPGPSDPYLRE  89
PBP  DELGKVLTPTQVKNRPT.STTWDGLDPGKLYTLVLTDPDAPSRKDPKYRE  82
A5   IEEGKTYTPTELKFQP..RLDWNA.DPESFYTVLMICPDAPNRENPMYRS 104
OV16 VNLGNELTPTQVKNQPT.KVSWDA.EPGALYTLVMTDPDAPSRKNPVFRE 111
DKA1 VAMGNTLPTEKARSKPQFQFTENVPQDDDLFTLVMTDPDAPSKTDHKWSE 108

CEN  HLHWIVTDIPGTTDSSFGKEVVSY..EMPRPNIGIHRFVFLLFKQKKRGQ 137
PBP  WHHFLVVNMKGNNISS.GTVLSDYVGSGPPKGTGLHRYVWLVYEQEGPLK 131
A5   RLHWLVVNVPGLDIMK.GQPISEYFGPLPPKDSGIQRYLILVYQQSDKLD 153
OV16 WHHWLIINISGQNVSS.GTVLSDYWIRSTKRHRTSSLCILGL....... 152
DKA1 ECHLVECDLKLLNEATHETTLIEYMGPAPPKGSGPHRYVFLLYKQPKGVD 175

CEN  ....AMLSPPVVCRDGFNTRKFTQENELGLPVAAVF 169
PBP  CDEPILSNRSGDHRGKFKVASFRKKYELGAPVAGTC 167
A5   FDEKKMELSNADGHSNFDVMKFTQKYEMGSPVAGNI 189
OV16 ..................................... 152
DKA1 SSKFSKIKDRPNGTPATGVGKWAKENNLQLVASNFF 214
```

FIG. 5 The *cen* locus. *a*, Map of the *cen* genomic region carrying the *cen*-663 allele. The insertion site of the transposon Tam6 is shown, with *Eco*RI (E), *Xba*I (X) and *Bam*HI (B) sites. An internal Tam6 *Xba*I fragment was used in screening to isolate the 6.0-kb *Eco*RI fragment (cloned as pJAM2017) that segregated with the *cen* phenotype in plants carrying *cen*-663. An *Eco*RI site that only partly cut in genomic digests allowed isolation of pJAM2017. *b*, Structure of the *cen* gene and the insertion sites of the transposon-generated alleles. Exons are represented by boxes, shaded for coding and open for non-coding, with introns represented by horizontal lines. Triangles on vertical lines show the transposon insertion sites. The arrow shows the direction of transcription. *c*, Nucleotide sequence of the *cen* cDNA compiled from 5′ and 3′ RT–PCR products and comparison with the genomic sequence. The deduced amino-acid sequence from the longest ORF is shown below. *d*, Similar sequences to CEN using BLAST[29]. The amino-acid sequence (one-letter code) is given for regions (indicated by the amino-acid numbers on the right) of the deduced protein gene products of the four highest scores: phosphatidylethanolamine-binding protein (PBP) of rats[17,18], antennal 5 protein (A5) of *Drosophila*, 16K antigen from *Onchocerca volvulus* (OV16), and the *dkaI* gene product of yeast (DKA1)[23–26]. The small vertical arrows indicate three regions of the DKA1 sequence which have been left out to simplify the comparison.

METHODS. The 6.0-kb *Eco*RI fragment identified in *cen*-663 with Tam6 was isolated, ligated to lambda gt10 arms, packaged *in vitro* (Amersham RPN1713, N334L), and a library of about 150,000 recombinants was screened with a 4-kb *Xba*I fragment of Tam6 (ref. 20). One positive was isolated, subcloned as pJAM2017, which when mapped revealed an internal *Eco*RI site. The region flanking Tam6, a 2-kb *Acc*I–*Eco*RI fragment shown as a thicker line beneath the locus in *a*, was used to screen a lambda EMBL4 library of wild-type *Antirrhinum* DNA (provided by H. Sommer). From about 500,000 recombinants, 7 overlapping clones were isolated, which were used to construct a map of the genomic region. Insertion sites were determined by sequencing products from PCR on genomic DNA of each allele, with oligonucleotides to *cen* and a conserved oligonucleotide to the CACTA family of transposable elements[30]. The 6.5-kb *Eco*RI fragment, pJAM2018, contained the insertion sites of all alleles but did not identify any clones when used as a probe against a cDNA library constructed from RNA of young inflorescences of wild-type *Antirrhinum*[31]. Therefore, 200 bp flanking the *cen*-663 allele were sequenced and oligonucleotides designed in both directions for RT–PCR on RNA from wild-type and *cen* mutant inflorescences[20,32]. This identified a cDNA, subcloned as pJAM2020, originating from the region flanking the insertion in *cen*-663 which was not expressed in each of the alleles. Both the genomic and cDNA clones were sequenced. The 5′ end of the *cen* mRNA was determined using the 5′ RACE system (GibcoBRL). Although a 65-bp longer 5′ PCR product was found, most evidence indicated that the transcript shown is likely to be the major *cen* mRNA. First, competitive PCR suggested that the larger transcript was at least 10-fold lower in abundance; second, the proteins with similarity to CEN (including that from the cDNA isolated from *Arabidopsis*) do not have such a long extension; and finally, only the smaller transcript has a potential TATA box.

interact with GTP-binding proteins. Less extensive similarity was found to the A5 protein of *Drosophila*, the OV16 antigen of *Onchocerca volvulus*, and DKA1 of yeast[23–26]. The antennal protein A5 was isolated by differential screening, is expressed in subsets of olfactory hairs, and is possibly an odorant-binding protein. OV16 was identified as an antigen that is recognized by sera from individuals infected with the filarial parasite *O. volvulus*. The *DKA1* gene has been shown to suppress certain *cdc25* mutations in yeast when introduced at high copy number, and may interact with the pathway involving RAS (GTP-binding protein), adenylyl cyclase and membrane receptors of external stimuli. Mutants have only been generated for *DKA1*, and these have no phenotype.

The databases also revealed high similarity of *cen* to expressed sequence tags from *Arabidopsis* and rice. An *Arabidopsis* clone (129D7T7 from the *Arabidopsis* Biological Resource Center at Ohio State) was fully sequenced and showed 70% identity to *cen* at both the nucleotide and protein level, and preliminary data suggest that this is the *tfl* gene of *Arabidopsis* (manuscript in preparation). Our initial data suggest that the two rice clones (OSR29181A and OSS1946A, from the Rice Genome Research Project, Ibaraki, Japan) may have been derived from unspliced transcripts.

Expression of *cen* and *flo*

We have shown that *cen* normally acts to prevent *flo* expression in the apical meristem. To determine if this reflected its region of expression, we analysed the pattern of *cen* RNA by *in situ* hybridization (Fig. 3*f*). In mature, wild-type inflorescences the expression of *cen* was mostly limited to the region just below the apical meristematic dome, and was absent from the epidermal and outer cell layers. Traces of expression in the stem below the dome were limited to the region shown (Fig. 3*f*). Thus *cen* expression is subapical, and does not significantly overlap with the region of ectopic *flo* expression observed in the cen mutant, which occurs throughout the apical dome. These results indicate that *cen* acts at a distance to prevent *flo* expression in the apical dome, or that *cen* is below the level of direction in the apex. Expression of *cen* was detected in other tissues of wild-type plants by RT–PCR, but the significance of this has not yet been determined (data not shown).

As *cen* appears to regulate *flo* in the apical meristem, expression of *cen* should precede *flo*. To test this we looked at the timing of *cen* expression in relation to floral induction by collecting wild-type plants after 0, 1, 2, 4, 6 or 8 days of induction. RNA *in situ* hybridization analysis revealed that *cen* expression was not seen until 4 days, even though *flo* was induced in axillary meristems by 1–2 days. This raised the possibility that, in addition to acting upstream to *flo*, some aspects of *cen* might be downstream of *flo*. To test this, young inflorescence apices from flo mutant plants were probed for *cen* expression. Plants carrying the *flo*-640 allele, which produces non-functional *flo* RNA, showed no *cen* expression by RNA *in situ* hybridization (data not shown). Control sections probed with *flo* confirmed earlier analysis, that *flo*-640 RNA was present in young bract primordia and weakly in the dome of the apical meristem[11]. It is therefore surprising that *flo* appears to be required for the expression of *cen* in the shoot apical meristem.

Models of inflorescence development

The architecture of the *Antirrhinum* inflorescence reflects the way in which *flo* and *cen* expression are coordinated. In flo mutants, flowers are replaced by indeterminate, continually branching shoots, whereas in cen mutants, the shoot is abruptly terminated by conversion to a flower. The gene expression studies suggest a model that accounts for the development of cen mutants and wild-type *Antirrhinum*.

In cen mutants, *flo* expression is activated within 1–2 days of floral induction (Fig. 6, *cen* day 2). Only the youngest initiating primordia are competent to form flowers, responding to the floral stimulus arriving at the apex. Older meristems remain vegetative, either because they do not receive the inductive signal or they are not competent to respond. The apical meristem of cen mutants does not express *flo* up to about day 4 and continues to grow, generating axillary meristems on its flanks. The growth rate of the apex appears similar to wild type during this period, by the rate of node initiation and pattern of cell division, based on analysis of histone expression[27]. However, by day 6, *flo* is expressed throughout the apical meristem, which is converted directly to a stage 2–3 floral meristem (Fig. 6). The ability of the apical meristem to be recruited to floral development at stages 2–3 contrasts with axillary meristems which cannot be recruited later than stage 0. This may be due to the inductive signal (or other factors) being spatially limited to the apical meristem.

There are two key features of this model that can account for additional aspects of the cen phenotype. First, the delayed activation of *flo* in the apical meristem allows several axillary meristems to be generated that give rise to flowers (usually 10). Second, the apical meristem is recruited at an advanced stage to become a stage 2–3 floral meristem. Expression of *flo* occurs throughout the meristem, and primordia that have already been initiated are recruited to form the sepals of the terminal flower. This suggests why the terminal flower is more advanced than axillary flowers, because at the time the apex is recruited the most advanced axillary meristem is only at stage 1–2. It further explains the spiral phyllotaxy of the sepals often observed in the terminal flower, as these could have been initiated by the apical inflorescence meristem just before it was recruited to form the terminal flower. Their variable number may simply reflect how many primordia were recruitable at the time the apical meristem was converted to floral development. The effects on organ number and symmetry of the terminal flower may also be due to direct conversion to a stage 2–3 floral meristem, without passing through stages 0–1. The earlier stages may be required for establishing the correct organ number and dorsal–ventral symmetry[11,13].

In wild-type apices, *flo* expression is activated in axillary meristems within 1–2 days of floral induction, as it is in cen

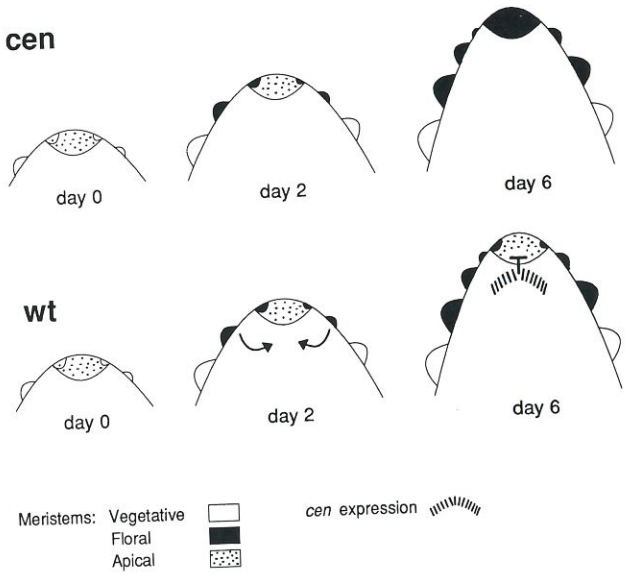

FIG. 6 Model for the early development of wild-type and cen mutant inflorescences of *Antirrhinum* upon floral induction. Diagrams show inflorescence apices on days 0, 2 and 6 after floral induction for the cen mutant and wild type. Axillary meristems develop from the flanks of the apical meristem. Floral meristems are indicated by black shading, apical meristems are dotted, and vegetative meristems have no shading. Bracts have been left out for clarity. In cen mutants, *flo* is activated in the apical meristem, but only after a delay. In wild type (wt), the arrows indicate signalling dependent on *flo* expression, leading to *cen* expression (line shading) in the sub-apical region of wild type. Activation of *cen* inhibits *flo* expression in the apical meristem.

mutants (Fig. 6, wild type day 2). During the next few days, further axillary meristems are generated by the apex, and these express *flo* and will give rise to flowers. No *cen* expression is observed in RNA *in situ* hybridization at this time (Fig. 6, day 2). However, by day 6, *cen* expression is found most strongly in the sub-apical region. Expression of *cen* appears to depend on the previous induction of *flo*, as RNA *in situ* analysis of young inflorescences of flo mutants indicated that they do not express *cen*. The possibility of a *flo*-independent pathway for the induction of *cen*, perhaps later in inflorescence development, awaits further analysis. Activation of *cen* inhibits apical *flo* expression, so that the meristem remains as an indeterminate inflorescence (Fig. 6, day 8). Expression of *flo* in axillary meristems is not inhibited by *cen*, either because *cen* action is spatially restricted or axillary meristems are less sensitive to *cen*. This model accounts for the observed ectopic accumulation of *flo* transcripts in the apex of flo mutants, as *cen* is not activated[11].

According to this model, *cen* and *flo* regulate each other non-autonomously. First, induction of *flo* activates *cen*, even though expression of *flo* is limited to axillary meristems and *cen* is activated in the sub-apical region. As these two regions do not overlap, this suggests that *flo* must signal across cells to activate *cen*. Second, in the cen mutant, *flo* is expressed ectopically throughout the apical dome, even though *cen* is largely expressed below the dome and does not extend into the outer cell layers of the apex. Therefore *cen* represses *flo* in the wild-type apex by signalling across cells. How *flo* and *cen* act is not clear from their predicted proteins. The protein FLO may be a transcriptional activator and initiate a cascade of new gene activities that leads to cell–cell signalling[9]. In contrast, CEN may bind a lipid-like molecule or interact with GTP-binding proteins or the membrane. CEN may therefore mediate an inhibitory signal or prevent the flowering signal from reaching the apical meristem.

How might this model account for the evolution of indeterminate inflorescence architectures? One possibility is that the ancestral role of *cen* was to prevent flower initiation in vegetative meristems. The switch from vegetative to reproductive development would therefore have required repression of *cen*, leading to a determinate inflorescence. The indeterminate condition may have arisen by limiting *cen* activity to the apex after the reproductive switch, preventing the apical meristem from forming a flower. The ancestral role of *cen* in the control of flowering time may have been lost or may be masked by genetic redundancy in *Antirrhinum*. This predicts that ectopic expression of *cen* may prevent or reduce flowering. How widespread this mechanism is for the generation of different plant architectures will require the analysis of *cen* and *flo* homologues in other species, particularly those where cen-like mutants are available[5,14–16]. □

Received 7 November 1995; accepted 15 January 1996.

1. Weberling, F. *Morphology of Flowers and Inflorescences* (Cambridge Univ. Press, 1989).
2. Coen, E. A. *Rev. Pl. Physiol. Pl. molec. Biol.* **42,** 241–279 (1991).
3. Weigel, D. & Nilsson, O. *Nature* **377,** 495–550 (1995).
4. Mandel, M. A. & Yanofsky, M. F. *Nature* **377,** 522–524 (1995).
5. Coen, E. S. & Nugent, J. M. *Development* (suppl.) 107–116 (1994).
6. Stebbins, G. L. *Flowering Plants, Evolution above the Species Level* (Harvard Univ. Press, MA, 1974).
7. Kuckuck, H. & Schick, R. *Z. indukt. Abstanim. -u. Vereblehre* **56,** 51–83 (1930).
8. Stubbe, H. *Genetik und Zytologie von Antirrhinum L. sect Antirrhinum* (VEB Gustav Frischer, Jena, 1966).
9. Coen, E. S. *et al. Cell* **63,** 1311–1322 (1990).
10. Huijser, P. *et al. EMBO J.* **11,** 1239–1250 (1992).
11. Carpenter, R. *et al. Pl. Cell* **7,** 2001–2011 (1995).
12. Carpenter, R. & Coen, E. S. *Genes Dev.* **4,** 1483–1493 (1990).
13. Coen, E. S. & Meyerowitz, E. M. *Nature* **353,** 31–37 (1991).
14. Keeble, F., Pellew, C. & Jones, W. N. *New Phytol.* **9,** 68–77 (1910).
15. Shannon, S. & Meeks-Wagner, D. R. *Pl. Cell* **3,** 877–892 (1991).
16. Alvarez, J., Guli, C. L., Yu, X.-H. & Smyth, D. R. *Pl. J.* **2,** 103–116 (1992).
17. Grandy, D. K. *et al. Molec. cell Endocr.* **4,** 1370–1376 (1990).
18. Bucquoy, S., Jolles, P. & Schoentgen, F. *Eur. J. Biochem* **225,** 1203–1210 (1994).
19. Schwarz-Sommer, Z. *et al. EMBO, J.* **11,** 251–263 (1992).
20. Bradley, D., Carpenter, R., Sommer, H., Hartley, N. & Coen, E. *Cell* **72,** 85–95 (1993).
21. Coen, E. S., Robbins, T. P., Almeida, J., Hudson, A. & Carpenter, R. in *Mobile DNA* (eds Berg, D. E. & Howe, M. M.) 413–416 (American Society for Microbiology, Washington DC, 1989).
22. Jameson, B. & Wolf, H. *Comput. Appl. Biosci.* **4,** 181–186 (1988).
23. Pikielny, C. W., Hasan, G., Rouyer, F. & Rosbash, M. *Neuron* **12,** 35–49 (1994).
24. Lobos, E. *et al. Molec. Biochem. Parasitol.* **39,** 135–146 (1990).
25. Tripp, M. L., Bouchard, R. A. & Pinon, R. *Molec. Microbiol.* **3,** 1319–1327 (1989).
26. Robinson, L. C. & Tatchell, K. *Molec. gen. Genet.* **230,** 241–250 (1991).
27. Fobert, P. R., Coen, E. S., Murphy, G. J. P. & Doonan, J. H. *EMBO J.* **13,** 616–624 (1994).
28. Williams, M. H. & Green, P. B. *Protoplasma* **147,** 77–79 (1988).
29. Altschul, S. F., Gish, W., Miller, W., Myers, E. W. & Lipman, D. J. *J. molec. Biol.* **215,** 403–410 (1990).
30. Luo, D., Coen, E. S., Doyle, S. & Carpenter, R. *Pl. J.* **1,** 59–69 (1991).
31. Simon, R., Carpenter, R., Doyle, S. & Coen, E. *Cell* **78,** 99–107 (1994).
32. Frohman, M. A., Dush, M. K. & Martin, G. R. *Proc. natn. Acad. Sci. U.S.A.* **85,** 8998–9002 (1988).
33. Bradley, D., Vincent, C., Carpenter, R. & Coen, E. *Development* (in the press).
34. Hammer, K., Knüpffer, S. & Knüffer, H. *Kulturpflanze* **38,** 91–117 (1990).

ACKNOWLEDGEMENTS. We thank N. Hartley for sequencing of the genomic region of *cen*; P. Walker for care and maintenance of plants; Z. Ladbrook, G. Ingram and R. Waites for help with the plants in the summer; and P. Cubas, E. Schultz and R. Simon for comments and discussions. This work was supported by BBSRC PMB2 and Stem Cell Programmes, the EEC AMICA Programme and the Gatsby Foundation.